HHS Public Access

Author manuscript

Ophthalmol Retina. Author manuscript; available in PMC 2019 July 01.

Published in final edited form as:

Ophthalmol Retina. 2018 July ; 2(7): 712–719. doi:10.1016/j.oret.2017.11.001.

Swept-Source OCT Angiography of Serpiginous Choroiditis

Kaivon Pakzad-Vaezi, MD[1], **Kosar Khaksari, PhD**[2], **Zhongdi Chu, MSc**[2], **Russell N Van Gelder, MD, PhD**[1,3,4], **Ruikang K Wang, PhD**[1,2], and **Kathryn L Pepple, MD, PhD**[1]

[1]Department of Ophthalmology, University of Washington, Seattle, WA 98104

[2]Department of Bioengineering, University of Washington, Seattle, WA 98195

[3]Department of Pathology, University of Washington, Seattle, WA 98195

[4]Department of Biological Structure, University of Washington, Seattle, WA 98195

Abstract

Purpose—To examine and quantify choriocapillaris lesions in active and quiescent serpiginous choroiditis (SC) using swept-source optical coherence tomography angiography (SS-OCTA) and en-face image analysis.

Design—Prospective observational case series.

Participants—Patients with a clinical diagnosis of SC.

Methods—A SS-OCTA prototype was used to image active and quiescent serpiginous lesions longitudinally before and after anti-inflammatory treatment. En-face slabs of choriocapillaris flow (CC-slab) or outer nuclear layer structure (ONL-slab) were generated from OCTA and OCT data, respectively.

Main Outcome Measures—Qualitative and quantitative analyses on lesion boundary and area using a semi-automated MATLAB algorithm. Lesions were also compared to traditional multimodal imaging

Results—Six eyes of three patients were imaged. Choroidal lesions were identified and analyzed in four of six eyes. Lesions with well-defined boundaries were identified in the CC-slab in areas of both active and inactive choroiditis. CC-slab lesion size and shape showed good correlation with lesions identified on indocyanine green angiography. CC-slab lesion area increased with disease activity and decreased with corticosteroid treatment. During active disease, the CC-slab lesion area was larger than both the ONL-slab and fundus autofluorescence lesion areas. Active CC-slab lesions not associated with corresponding abnormal autofluorescence resolved without clinical

Corresponding Author: Kathryn L Pepple, MD, PhD, 908 Jefferson St, Seattle, WA, 98104, Phone: 206-897-4611, Fax: 206-897-4320, kpepple@u.washington.edu.

Conflict of Interest:

No conflicting relationship exists for authors KPV, KK, ZC, RNVG, or KLP:

This article contains additional online-only material. The following should appear online-only: Figures 2, 4, and 6.

scarring after treatment. In inactive scars, the areas of retinal and choriocapillaris lesions were similar and did not change over time.

Conclusions—En-face analysis of SS-OCTA choriocapillaris flow voids provide a non-invasive method for the detection of lesions in patients with SC. The presence of lesions in the choriocapillaris in the absence of retinal pigment epithelium and outer retinal abnormalities supports the hypothesis that choriocapillaris is the primary site of pathology in SC, and may be a sensitive early sign of disease activity. We propose a simple grading system of SC lesions based on SS-OCTA and fundus autofluorescence findings. SS-OCTA is a promising non-invasive method for monitoring patients with SC.

Serpiginous choroiditis (SC) is a rare form of bilateral, chronic or recurrent posterior uveitis that is thought to primarily involve the choriocapillaris, with subsequent involvement of the retinal pigment epithelium (RPE), and outer retina.[1–3] It causes severe permanent vision loss when involving the fovea and parafovea. This has led to a practice pattern of initiating aggressive immunosuppressive treatment (IMT) upon diagnosis, with evidence of progressive expansion of old lesions, or with identification of new lesions.[1,4,5] The identification of disease activity prior to permanent structural damage would provide the opportunity to prevent vision loss.

Currently, SC is diagnosed based on clinical appearance and characteristic changes of active lesions using fluorescein angiography (FA),[1,6] with indocyanine green angiography (ICGA) as an adjunct that can identify subclinical lesions.[7,8] Both these studies suggest a primary inflammatory pathology at the level of the choriocapillaris. Fundus autofluorescence (FAF) has more recently been reported to highlight active lesions with foci of hyper-autofluorescence, presumably reflecting acute RPE injury overlying the choriocapillaris inflammation.[9] Inactive scars on the other hand become hypo-autofluorescent.[1,6,8] However, none of these modalities provide high resolution imaging of the choriocapillaris, which appears to be fundamentally affected in SC.

Optical coherence tomography angiography (OCTA) has emerged as a non-invasive imaging modality to detect the presence or absence of blood flow signal in the retina.[10] Unlike dye-based angiography methods, OCTA allows vascular analyses to be stratified by retinal layer. OCTA has provided insights into pathogenic mechanisms of retinal disease, including uveitic conditions.[11] Compared with dye angiography, OCTA also has the benefit of providing high resolution digital images that are amenable to reproducible quantification.

Most currently available OCTA devices utilize spectral-domain (SD) OCT technology. Unfortunately, diseases of the choroid and choriocapillaris are difficult to study with SD technology due to RPE attenuation of the 840 nm central wavelength used in this imaging modality.[12] Despite this limitation, SD-OCTA has identified flow voids in the choroid of patients with placoid chorioretinal diseases such as acute posterior multifocal placoid pigment epitheliopathy (APMPPE).[13] Swept-source (SS) OCT and OCTA utilize a longer central wavelength (1050 nm) that provides improved signal penetration through the RPE and produces high resolution images of the choriocapillaris and choroidal vessels.[14,15] Swept-source technology OCTA has the potential to provide the benefits of non-invasive

vascular imaging to identify and monitor diseases that are believed to originate in the choriocapillaris.

In this study we sought to examine the utility of SS-OCTA to detect choriocapillaris involvement in patients with SC. Furthermore, we compared SS-OCTA with other standard imaging modalities including FA, ICGA, SD-OCT, and FAF to determine their relative utility in characterization of active and quiescent SC.

Methods

This single-institution prospective observational case series was approved by the Institutional Review Board at the University of Washington. Patients with a diagnosis of peripapillary SC, macular SC, or multifocal/"ampiginous" choroidopathy were recruited for OCTA imaging as part of this study between September 2016 to March 2017. Informed consent was obtained, and the tenets of the Declaration of Helsinki and the Health Insurance Portability and Accountability Act of 1996 regulations were followed.

SS-OCTA and SS-OCT images were obtained using a PLEX® Elite 9000 (Carl Zeiss AG, Dublin, California). This device uses a central wavelength of 1050-nm with 100-kHz A-scan rate and a spectral bandwidth of 100-nm. The axial and lateral resolutions are ~5 μm and ~14 μm, respectively. An optical microangiography (OMAG©) algorithm was used to construct images demonstrating surrogate markers of vascular flow, the technical aspects of which are detailed elsewhere.[16] Fields of view sizes included 3mm × 3mm, 6mm × 6mm, 9mm × 9mm, and 12mm × 12mm imaging windows. A 3mm × 3mm cube contains 300 A-scans per B-scan, and a total of 1200 B-scans, 4 repeats each, while the 6mm × 6mm, 9mm × 9mm and 12mm × 12mm cubes hold 500 A-lines per B-scan, with a total of 1000 B-scans, 2 repeats, centered at the fovea or the optic disc. Pixel spacing and the number of repeated B-scans were compromised in larger scans to maintain similar scanning time as 3×3.The specific scanning window size chosen for analysis was selected based on the size and location of the region containing pathology. OCTA images of the choriocapillaris slab (CC-slab) (measured from 15 to 35 μm below the RPE best fit line), OCT images of RPE slab (from 0 to 10 μm anterior to the RPE best-fit line) and OCT images of the outer nuclear slab (ONL-slab) (from 55 to 105 μm anterior to the RPE best-fit line) were then generated for en-face analysis for the same field of view. A semi-automated MATLAB algorithm was used to identify and measure lesion area on the en-face slabs. Lesion area was determined manually by one expert grader with fellowship training in both medical retina and uveitis (KPV), area was calculated, and the lesions in the various slabs were then overlaid for comparison.

Clinical images were collected for comparison with OCT and OCTA research images. Clinical images were ordered at the discretion of the treating physician and included color fundus photography (FF450Plus, Carl Zeiss AG, Dublin, California), spectral-domain OCT (Spectralis HRA+OCT, Heidelberg Engineering, Heidelberg, Germany), FAF (FF450Plus, Carl Zeiss AG; Spectralis HRA+OCT, Heidelberg Engineering), FA (FF450Plus, Carl Zeiss AG; P200DTx, Optos PLC, Dunfermline, Scotland, United Kingdom), and ICG angiography (Spectralis HRA+OCT, Heidelberg Engineering). ICGA and FAF images for Patient 1 were

exported as TIFF image files and analyzed using the semi-automated MATLAB algorithm to determine lesion size.

Patients were diagnosed with serpiginous choroiditis after an evaluation for other infectious and inflammatory etiologies that included a careful uveitis review of systems and laboratory testing with a complete blood count, comprehensive metabolic panel, *Treponema pallidum* IgG and IgM for syphilis, an interferon-gamma release assay for tuberculosis (QuantiFERON-TB Gold®), and a chest x-ray. A complete ophthalmic examination was performed, and uveitis was categorized according to Standardization of Uveitis Nomenclature criteria.[17] Initial treatment consisted of an oral tapering course of corticosteroid with concomitant IMT, consistent with expert consensus recommendations.[18]

Results

Three patients were identified with SC: Patient 1 with macular SC, Patient 2 with classic peripapillary SC, and Patient 3 with multifocal SC. Patient 1 was a 55 year-old Caucasian male with a 3-month history of central scotoma and photopsias in the left eye. Fundus imaging, FAF, FA, ICGA, and SS-OCTA were performed (Figure 1) and he was diagnosed with macular SC of the left eye after the evaluation for infectious and inflammatory conditions. The right eye had mild peripapillary atrophy (not shown). Late ICGA images were used to outline the region of choriocapillaris defect and quantify the area involved in the left eye (Figure 1D). The total area of CC defect detected by ICGA was determined to be 17.4 mm^2 (Table 1). The lesion shape in the CC-slab approximated the ICGA boundary, and lesion area was similar at 17.5 mm^2. The ONL-slab boundary fell within the boundary of the CC lesion (Figure 1G), and the lesion area was smaller (14.4 mm^2). The RPE lesion, as identified by FAF demonstrated, a similar shape as the CC lesion (Figure 1H), and the lesion area was similar (17.6 mm^2).

Patient 2 was a 41 year-old Caucasian male with a 4-month history of scotoma and photopsia in his left eye. He had been diagnosed with probable serpiginous choroiditis prior to presentation, but had not received any treatment. On exam, an inactive serpiginoid scar extending from the optic nerve into the macula was noted in the right eye (Figure 2A,C - available at http://www.ophthalmology-retina.org). In the left eye there was concern for an area of active peripapillary choroiditis that demonstrated late leakage on fluorescein angiography and hyper-autofluorescence at the superotemporal optic nerve border (Figure 2 - available at http://www.ophthalmology-retina.org). Treatment with prednisone and mycophenolate mofetil was initiated, but during the prednisone taper at 10 mg daily, he experienced a recurrence in the left eye (Figure 3F). Oral corticosteroids were increased and tacrolimus started, and the flare was controlled (Figure 3K). On the CC-slab, the area of the lesion nasal to the retinal vessels did not change in boundary or area over the three visits (Figure 3C,H,M red dotted lines). There was also no change in the ONL-slab in this region (Figure 3D,I,N green dotted lines) or the appearance on FAF (Figure 3B,G,L). In this area, the boundary of the lesion as defined by all three imaging modalities was closely aligned and the total area involved did not change. This area was considered an inactive scar. In contrast, the temporal aspect of the CC-slab lesion expanded in size (Figure 3H solid red line). In comparison to the clinical fundus images, the CC-slab lesion had sharply delineated

borders. The area of ONL disruption also expanded during the flare, but involved less area than the CC-slab lesion (Table 1) (Figure 3I–J). The FAF lesion did not demonstrate expansion of significant hyper-autofluorescence, but subtle stippled hyper-autofluorescence was noted in the area overlying the CC-slab lesion (Figure 3G). After additional treatment with pulse oral prednisone and tacrolimus dose increase, the lesion became quiescent on clinical exam (Figure 3K) and the CC and ONL lesion areas decreased in size (Figure 3M–O). In contrast, the area of hyper-autofluorescence expanded, and developed a hypo-autofluorescent rim (Figure 3L).

Patient 3 was a 21 year-old Caucasian female who presented with 3 weeks of worsening floaters, photopsias, and central scotomata in her right eye. Fundus imaging, FA, and ICGA were performed (Figure 4 - available at http://www.ophthalmology-retina.org), leading to a diagnosis of multifocal SC in the right eye after the evaluation for infectious and inflammatory conditions. The left eye was minimally affected with one perifoveal lesion (Figure 4B - available at http://www.ophthalmology-retina.org). Triple therapy with prednisone, azathioprine, and tacrolimus was initiated. Despite favorable clinical response to therapy, she developed a significant tremor that responded to discontinuation of tacrolimus. She returned 3 weeks later with new photopsias and new macular lesions were noted in the right eye (Figure 5A arrows). FAF imaging showed that one lesion was hyper-autofluorescent (Figure 5B white arrow) while the adjacent lesion showed minimal FAF changes (Figure 5B black arrow). SS-OCTA obtained at this visit demonstrated very well-defined lesions in the CC-slab associated with the two new clinically apparent lesions (Figure 5C). In addition, multiple small lesions along and beyond the superior arcade were identified that were otherwise not appreciated by routine clinical exam or imaging (Figure 5C circles). Outer retinal layer abnormalities were also identified on the ONL-slab that corresponded to the clinically apparent lesions (Figure 5D,E), but no ONL abnormalities were seen in association with the small lesions superior to the vascular arcade noted only on the CC-slab. Tacrolimus was re-started, as were oral corticosteroids with a burst and taper schedule. With treatment, the visible lesions resolved clinically and evolved into early scars with the development of hypo-autofluorescence on FAF (Figure 5I,J). On follow-up, two patterns of CC flow void changes were noted. The larger lesion associated with FAF changes decreased in size, but persistent flow abnormalities in the choriocapillaris remained (Figure 5K white and black arrowheads and 5N-P areas in red). The ONL-slab abnormality associated with the clinically visible and hyper-autofluorescence lesion also decreased in size, but did not resolve completely (Figure 5M white arrowhead and 5N-P areas in green). In contrast, the small lesions seen only in the CC-slab outside the superior arcade resolved completely.

Discussion

This series of patients with SC illustrates the potential utility of SS-OCTA as a modality for detecting and monitoring choriocapillaris lesions. This non-invasive modality mirrored ICGA findings in one patient with inactive disease, and provided increased sensitivity for detection of new lesions compared with FAF in two patients with active disease.

OCTA imaging in Patient 1 demonstrated the ability of this technique to non-invasively identify clinically relevant choriocapillaris lesions that were also present on ICGA, with high agreement on lesion size and location. In Patient 2, OCTA demonstrated the presence of a well-defined choriocapillaris lesion that increased in area during a disease flare, and decreased in area with corticosteroid treatment. Interestingly, hyper-autofluorescence of the new lesion on FAF imaging did not develop until after steroid treatment was initiated and after the CC-slab lesion had already decreased in size. This suggests that FAF imaging may not be as sensitive a non-invasive imaging marker of acute disease as OCTA.[6,9,19] In both Patients 2 and 3, several new lesions failed to induce marked FAF changes despite clearly visible lesions in the CC-slab and the ONL-slab. Furthermore, in both patients, after treatment was initiated, the CC-slab and ONL-slab lesions decreased in size, but the hyper-autofluorescent lesion grew or developed hypo-autofluorescence and scarring. This suggests that FAF may lag choriocapillaris-level pathology, as would be the case if the RPE (source of FAF signal) were indirectly injured following a primary insult to the CC. In contrast, in Patient 1 (who had delayed diagnosis and treatment for at least 3–4 months after the initial symptoms) the area of the CC-lesion and FAF lesion were very similar in size. This disparity suggests that prompt and aggressive treatment provides the opportunity to reverse to some extent the damage to the choriocapillaris and prevent overlying retinal and RPE damage.

Considered to be one of the “placoid” chorioretinopathies, SC classically originates and expands from a peripapillary location in a serpiginoid fashion from single or multiple initial lesions. However, there are variations that do not have a peripapillary component and are termed “macular serpiginous”, or that are noteworthy for the number of lesions termed “multifocal serpiginous”, or that initially have a benign appearance similar to APMPPE but develop a relentlessly progressive course, termed “ampiginous choroiditis”.[1,6,8,20,21] Despite autoimmune, infectious, vascular, and degenerative hypotheses proposed, no cause has been definitively determined.[1,22] It is thought that SC originates in the choriocapillaris, with secondary effects on the RPE and retina, leading some to call it a “choriocapillaropathy”.[8] Rare histopathologic studies have demonstrated atrophy of all three layers, but support the hypothesis that the choriocapillaris is involved primarily.[20,23] Studies with ICGA suggest a flow void in the choriocapillaris, with better delineation of lesions and often a larger area of involvement than seen on FA or clinical exam.[1,6,7,24,25] Subclinical hypofluorescent lesions on ICGA can be detected prior to RPE or retinal changes.[7] However, access to these tests, particularly ICGA, may be limited, and their invasive nature combined with the need for repeated imaging, presents a risk/benefit/cost profile that may be unacceptable. Non-invasive choriocapillaris imaging in placoid chorioretinopathies will advance both our understanding of disease pathogenesis and assist in management decisions. While not including patients with SC, Klufas et al[13] recently described spectral-domain OCTA findings in patients with APMPPE, persistent placoid maculopathy, and relentless placoid chorioretinitis. They showed areas of absent flow signal on OCTA using a split-spectrum amplitude-decorrelation angiography (SSADA) algorithm at the level of the choriocapillaris that were typically larger than corresponding areas on FA, and either the same or larger than ICG lesions. Outer retina structural OCT demonstrated disruption that colocalized with acute choriocapillaris lesions that decreased in size either spontaneously or with treatment.

Our findings in SC also implicate the choriocapillaris as the primary site of pathology. Our data suggest that lesions seen on the CC-slab represent flow voids rather than blockage due to the consistent signal penetration to deeper structures in regions with and without clinical lesions, and the absence of shadowing on the B-scans used to generate the en-face slabs (Figure 6 - available at http://www.ophthalmology-retina.org). These findings, in conjunction with delayed damage identified on FAF to overlying RPE, suggest an ischemic event at the level of the CC rather than inflammatory infiltrate, which would block light signal at deeper levels. Slow blood flow beyond detection limits, however, could not be differentiated from complete lack of flow with current technology used in this study. Despite this, our data also suggests that the most acute lesions appear as flow voids on OCTA, and may have the potential for rapid and complete resolution when treatment is instituted promptly. However, when outer retinal changes develop as identified by the ONL-slab abnormalities, and particularly when RPE damage causes FAF changes, permanent scars may be more likely to develop.

Using SS-OCTA together with other non-invasive imaging modalities, we suggest SC lesions can be characterized by grades that are based on characteristic multimodal imaging findings (Table 2). Grade 1 lesions are characterized by the presence of abnormalities at the level of the choriocapillaris as seen by CC-slab lesions without ONL-slab abnormalities or FAF changes. Grade 2 lesions have progressed to involve not only the choriocapillaris, but also the overlying outer retina, and can be identified by the presence of abnormalities in both the CC-slab and ONL-slab. In more acute lesions, the CC-slab area typically will encompass and extend beyond the ONL-slab lesion area. However, in the absence of treatment, the areas of the CC and ONL lesion overlap will increase, along with increased border alignment. Grade 3 lesions correspond to subacute to chronic disease activity that has led to RPE dysfunction and ultimately scarring. Grade 3 lesions can be identified by the presence of FAF abnormalities (sub-acute with hyper-autofluorescence, chronic with hypo-autofluorescence) in addition to CC-slab and ONL-slab lesions. This grading system has potential clinical importance based on our data suggesting that with prompt treatment, Grade 1 and to some extent Grade 2 lesions may resolve without subsequent RPE damage or permanent scar formation. We propose this preliminary grading system to assist future studies by providing a systematic approach and consistent language to describe the evolution of acute serpiginous choroiditis lesions. However, due to the limited number of cases presented here, the grading system will require validation with a larger number of cases.

Limitations of this study include the small number of patients, limited follow-up, and limited comparison of OCTA to the traditional standard of ICGA. It is likely that ICGA would detect some or all of the lesions found on SS-OCTA,[7,8,24] however due to the risks associated with an invasive test, it was not performed when the treating clinician at our institution believed that management would not change. Future study should seek to validate SS-OCTA against traditional ICGA with a prospective study design. Artifacts have been identified in previous studies using SD-OCTA,[26] and have the potential to influence imaging and quantitation of the deeper choroidal structures. Shadowing from overlying retinal structures could lead to false attribution of choroidal flow voids. However, this was not identified as a significant factor in a previous study[13] or in the work presented here. These and other issues such as motion artifact will become less of a concern for future studies with

improved image processing.[27–29] This study also benefitted from the increased scanning speeds provided by a swept-source system, as we were able to obtain images over larger areas of the fundus than were previously possible. The ability to image the entire macula will be particularly useful to detect subclinical lesions that may not be noticed by patients or other imaging systems due to their extrafoveal location. Ongoing study of the clinical relevance of SS-OCTA images will help clarify the utility of this modality.

The current era of advanced *in vivo* imaging allows detection of acute and subclinical lesions in diseases like SC. Symptoms, or the lack thereof, may not reflect active pathology as demonstrated on sensitive imaging modalities. The potential for identification of lesions with rapid, non-invasive imaging may provide clinicians with a window of opportunity to prevent permanent retinal damage.

Supplementary Material

Refer to Web version on PubMed Central for supplementary material.

Acknowledgments

Financial Support: This work was supported by NIH Core Grant P30EY001730 (RNVG), Carl Zeiss Meditec Inc and National Eye Institute R01 EY024158 (RKW), K08 EY023998 (KLP), an unrestricted departmental grant from Research to Prevent Blindness, the Cynthia and Joseph Gensheimer Fellowship (KPV), and the Mark J. Daily, MD Ophthalmology Research Fund. The sponsor or funding organizations had no role in the design or conduct of this research.

For author RKW: received research support from Carl Zeiss Meditec Inc., Tasso Inc. and Colgate Palmolive Company. Dr. Wang and the Oregon Health and Science University co-own a patent that is licensed to Carl Zeiss Meditec Inc. and Kowa Inc. He is a consultant to Insight Photonic Solutions.

Abbreviations

SC	serpiginous choroiditis
SS	swept-source
SD	spectral-domain
OCTA	optical coherence tomography angiography
OCT	optical coherence tomography
CC	choriocapillaris
ONL	outer nuclear layer
RPE	retinal pigment epithelium
IMT	immunosuppressive treatment
FA	fluorescein angiography
FAF	fundus autofluorescence
ICGA	indocyanine green angiography

APMPPE	acute posterior multifocal placoid pigment epitheliopathy
OMAG	optical microangiography
SSADA	split-spectrum amplitude-decorrelation angiography

References

1. Lim W-K, Buggage RR, Nussenblatt RB. Serpiginous choroiditis. Surv Ophthalmol. 2005; 50:231–244. [PubMed: 15850812]
2. Laatikainen L, Erkkilä H. A follow-up study on serpiginous choroiditis. Acta Ophthalmol. 1981; 59:707–718. [PubMed: 6171987]
3. Gass JDM. Stereoscopic atlas of macular diseases: diagnosis and treatment. 3. St Louis, MO; Mosby: 1987.
4. Christmas NJ, Oh KT, Oh DM, Folk JC. Long-term follow-up of patients with serpinginous choroiditis. Retina. 2002; 22:550–556. [PubMed: 12441719]
5. Hooper PL, Kaplan HJ. Triple agent immunosuppression in serpiginous choroiditis. Ophthalmology. 1991; 98 944-951-952.
6. Nazari Khanamiri H, Rao NA. Serpiginous choroiditis and infectious multifocal serpiginoid choroiditis. Surv Ophthalmol. 2013; 58:203–232. [PubMed: 23541041]
7. Giovannini A, Ripa E, Scassellati-Sforzolini B, Ciardella A, Tom D, Yannuzzi L. Indocyanine green angiography in serpiginous choroidopathy. Eur J Ophthalmol. 1996; 6:299–306. [PubMed: 8908438]
8. Bouchenaki N, Cimino L, Auer C, Tao Tran V, Herbort CP. Assessment and classification of choroidal vasculitis in posterior uveitis using indocyanine green angiography. Klin Monatsbl Augenheilkd. 2002; 219:243–249. [PubMed: 12022010]
9. Yeh S, Forooghian F, Wong WT, et al. Fundus autofluorescence imaging of the white dot syndromes. Arch Ophthalmol. 2010; 128:46–56. [PubMed: 20065216]
10. Spaide RF, Klancnik JM, Cooney MJ. Retinal vascular layers imaged by fluorescein angiography and optical coherence tomography angiography. JAMA Ophthalmol. 2015; 133:45–50. [PubMed: 25317632]
11. Kim AY, Rodger DC, Shahidzadeh A, et al. Quantifying retinal microvascular changes in uveitis using spectral-domain optical coherence tomography angiography. Am J Ophthalmol. 2016; 171:101–112. [PubMed: 27594138]
12. Miller AR, Roisman L, Zhang Q, et al. Comparison between spectral-domain and swept-source optical coherence tomography angiographic imaging of choroidal neovascularization. Invest Ophthalmol Vis Sci. 2017; 58:1499–1505. [PubMed: 28273316]
13. Klufas MA, Phasukkijwatana N, Iafe NA, et al. Optical coherence tomography angiography reveals choriocapillaris flow reduction in placoid chorioretinitis. Ophthalmology Retina. 2017; 1:77–91.
14. Moult EM, Waheed NK, Novais EA, et al. Swept-source optical coherence tomography angiography reveals choriocapillaris alterations in eyes with nascent geographic atrophy and drusen-associated geographic atrophy. Retina. 2016; 36(Suppl 1):S2–S11. [PubMed: 28005659]
15. Mrejen S, Spaide RF. Optical coherence tomography: imaging of the choroid and beyond. Surv Ophthalmol. 2013; 58:387–429. [PubMed: 23916620]
16. Zhang A, Zhang Q, Chen C-L, Wang RK. Methods and algorithms for optical coherence tomography-based angiography: a review and comparison. J Biomed Opt. 2015; 20:100901. [PubMed: 26473588]
17. Jabs DA, Nussenblatt RB, Rosenbaum JT. Standardization of Uveitis Nomenclature (SUN) Working Group. Standardization of uveitis nomenclature for reporting clinical data. Results of the First International Workshop. Am J Ophthalmol. 2005; 140:509–516. [PubMed: 16196117]
18. Jabs DA, Rosenbaum JT, Foster CS, et al. Guidelines for the use of immunosuppressive drugs in patients with ocular inflammatory disorders: recommendations of an expert panel. Am J Ophthalmol. 2000; 130:492–513. [PubMed: 11024423]

19. Cardillo Piccolino F, Grosso A, Savini E. Fundus autofluorescence in serpiginous choroiditis. Graefes Arch Clin Exp Ophthalmol. 2009; 247:179–185. [PubMed: 18802719]
20. Hardy RA, Schatz H. Macular geographic helicoid choroidopathy. Arch Ophthalmol. 1987; 105:1237–1242. [PubMed: 3632442]
21. Gupta V, Agarwal A, Gupta A, Bambery P, Narang S. Clinical characteristics of serpiginous choroidopathy in North India. Am J Ophthalmol. 2002; 134:47–56. [PubMed: 12095807]
22. Pallin SL. Noninfectious posterior chorioretinopathies: curious multifocal and contiguous disorders. Ann Ophthalmol. 1977; 9:713–718. [PubMed: 911114]
23. Wu JS, Lewis H, Fine SL, Grover DA, Green WR. Clinicopathologic findings in a patient with serpiginous choroiditis and treated choroidal neovascularization. Retina. 1989; 9:292–301. [PubMed: 2483464]
24. Salati C, Pantelis V, Lafaut BA, Sallet G, De Laey JJ. A 8 months indocyanine angiographic follow-up of a patient with serpiginous choroidopathy. Bull Soc Belge Ophtalmol. 1997; 265:29–33. [PubMed: 9479817]
25. Squirrell DM, Bhola RM, Talbot JF. Indocyanine green angiographic findings in serpiginous choroidopathy: evidence of a widespread choriocapillaris defect of the peripapillary area and posterior pole. Eye (Lond). 2001; 15:336–338. [PubMed: 11450736]
26. Spaide RF, Fujimoto JG, Waheed NK. Image artifacts in optical coherence tomography angiography. Retina. 2015; 35:2163–2180. [PubMed: 26428607]
27. Camino A, Zhang M, Gao SS, et al. Evaluation of artifact reduction in optical coherence tomography angiography with real-time tracking and motion correction technology. Biomed Opt Express. 2016; 7:3905–3915. [PubMed: 27867702]
28. Hwang TS, Zhang M, Bhavsar K, et al. Visualization of 3 distinct retinal plexuses by projection-resolved optical coherence tomography angiography in diabetic retinopathy. JAMA Ophthalmol. 2016; 134:1411–1419. [PubMed: 27812696]
29. Zhang QQ, Zhang AQ, Lee C, et al. Projection artifact removal enables accurate presentation and monitoring of choroidal neovascularization imaged by optical coherence tomography angiography. Ophthalmology Retina. 2017; 1:124–136. [PubMed: 28584883]

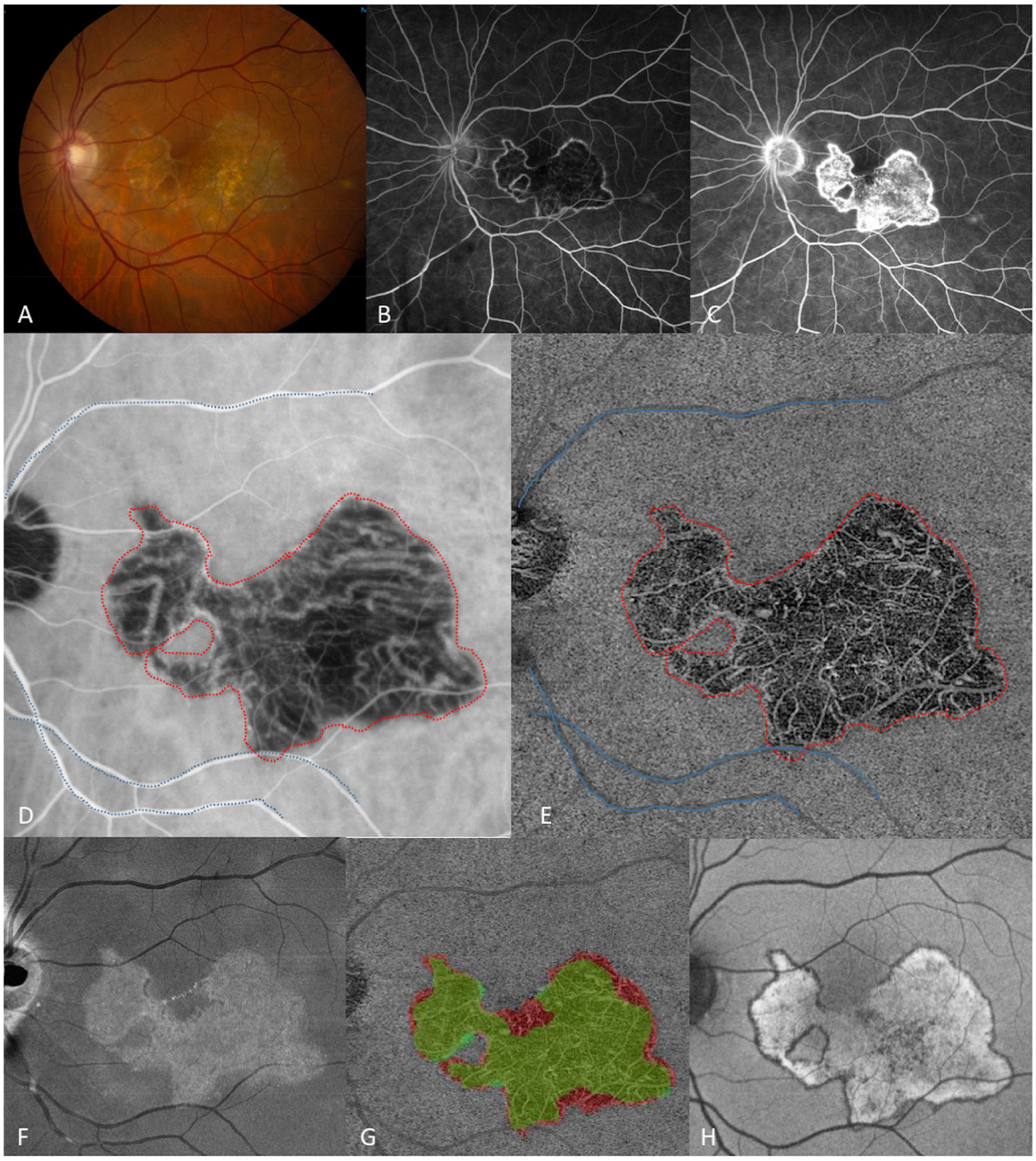

Figure 1.

Patient 1 at presentation, demonstrating an area of macular serpiginous choroidopathy in the left eye with well-defined borders and areas of retinal pigment epithelium atrophy (A). Fluorescein angiography showed early hypofluorescence (B), and late hyperfluorescence (C) of the central lesion. Late frames from indocyanine green angiography (ICGA) revealed hypofluorescence of the lesion (D). The en-face projection of the choriocapillaris slab obtained from swept-source optical coherence tomography angiography (SS-OCTA) demonstrated absent small vessel flow (E). The choriocapillaris lesion boundary and major blood vessel outlines were defined and grouped in the SS-OCTA image (D), and overlaid en-

bloc on the magnification-matched ICGA image (E) using MatLab software. The hyperreflective region seen in the en-face outer retinal slab (F) identified the area of retinal damage. Overlay of the larger choriocapillaris lesion (red) with the smaller outer retinal lesion (green, G). Fundus autofluorescence with diffuse central hyper-autofluorescence and a thin hypo-autofluorescent border (H).

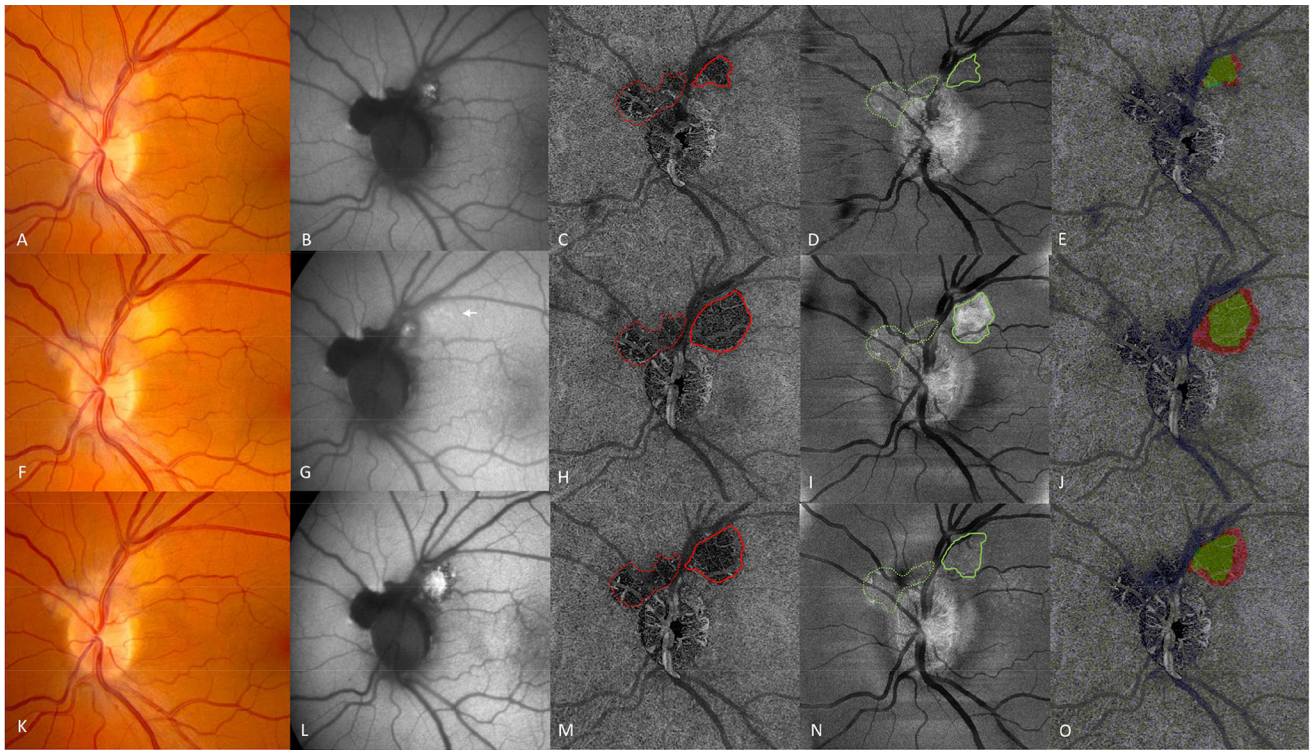

Figure 3.

Patient 2. First row: one month after initiation of prednisone and mycophenolate mofetil. Color fundus (A) and autofluorescence (B) images of an active lesion at the superotemporal disc margin. En face swept-source optical coherence tomography angiography (SS-OCTA) choriocapillaris (CC) slab (C) revealed flow voids associated with an inactive scar that did not change with time (dotted red line) and flow voids that changed with disease activity (solid red outline). The en face outer retinal slab (D) showed an area of bright hyperreflectivity in the area of scar (dotted green line), and less pronounced hyperreflectivity in the area of disease activity (solid green outline). Overlay (E) of the choriocapillaris lesion (red) and outer retina lesion (green). Second row: Disease flare. Arrows indicate new lesions by color fundus (F) and autofluorescence (G). En face SS-OCTA CC-slab (H) with lesion enlargement and well-defined borders (solid red outline). The en face outer retina slab (I) with a larger and brighter lesion (solid green outline). Overlay of the choriocapillaris lesion (red), and outer retinal lesion (green in J). Third row: After one month of tacrolimus and oral prednisone, decreased activity on color fundus (K) and increased autofluorescence (L). The SS-OCTA CC-slab (M) demonstrated reduced lesion area compared to H (solid red outline).The outer retinal slab (N) demonstrated decreased size and hyperreflectivity of the outer retinal lesion (solid green outline). Overlay of the choriocapillaris lesion (red), and outer retinal lesion (green in O).

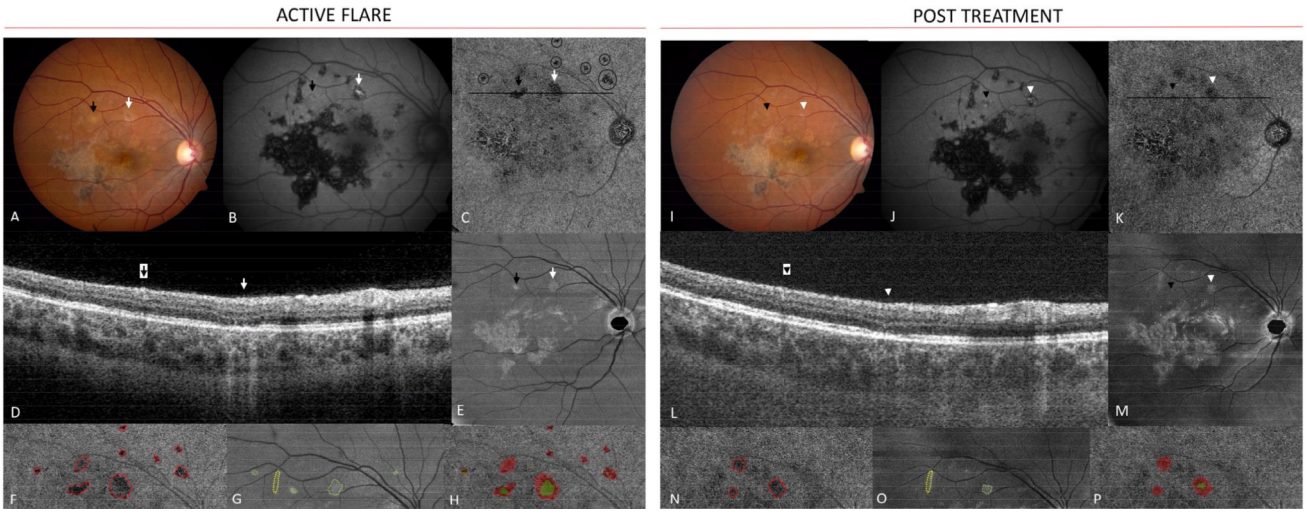

Figure 5.

Patient 3. Left: After discontinuation of tacrolimus, new lesions developed (arrows in A). One lesion demonstrated concurrent hyper-autofluorescence (white arrow, B). En face swept-source optical coherence tomography angiography (SS-OCTA) choriocapillaris (CC)-slab (C) revealed flow voids in the areas of the clinical lesions (arrows in C). Additional lesions were identified (circles in C) that were not clearly visible on color or fundus autofluorescence images (B). B-scan through the acute lesions (D). Outer retinal en face slab (E) with areas of hyperreflectivity corresponding to the clinically visible lesions. Magnified SS-OCTA CC-slab image (F) highlighting multiple CC lesions (red). Magnified outer retinal slab (G) with outer retinal lesions (green). Overlap of F and G (H). Right: After treatment with tacrolimus and prednisone, disease activity decreased on color images (I), and became more hypo-autofluorescent (J). Macular en face SS-OCTA CC-slab (K). B-scan (L) shows early recovery of the ellipsoid layer and decreased signal transmission (white arrowhead). Outer retinal slab (M). Magnified SS-OCTA CC-slab (N) and outer retinal slabs (O) show post treatment improvement in lesion size. Overlap of N and O (P). Prior scar (yellow) did not change before and after treatment (G, O).

Table 1

Serpiginous choroiditis lesion area in mm^2

	Case 1		Case 2			Case 3	
	Visit 1	**Visit 2**	**Visit 2**	**Visit 4**	**Visit 5**	**Visit 1**	**Visit 3**
Choriocapillaris *	17.5	18.8	0.42	1.48	1.17	3.30	1.50
Outer retina †	14.4	16.7	0.36	0.82	0.67	0.624	0.154
Choroid ††	17.4	-	-	-	-	-	-

*As imaged by swept-source optical coherence tomography angiography.

†As imaged by enface structural swept-source optical coherence tomography.

††As imaged by indocyanine green angiography on Spectralis HRA+OCT, Heidelberg Engineering.

Table 2

Serpiginous choroiditis lesion grade based on multimodal imaging.

	Anatomical involvement
Acute	
Grade 1	Choriocapillaris only *
Grade 2	Grade 1, plus Outer Retina †
Grade 3	Grade 2, plus Retinal Pigment Epithelium – hyperautofluorescence on fundus autofluorescence imaging
Chronic	Hypoautofluorescence on fundus autofluorescence

* as imaged by swept-source optical coherence tomography angiography or indocyanine green angiography.

† as imaged by optical coherence tomography.